HHS Public Access

Author manuscript

Cell. Author manuscript; available in PMC 2016 January 29.

Published in final edited form as:

Cell. 2015 January 29; 160(3): 503–515. doi:10.1016/j.cell.2015.01.011.

Identification of a spinal circuit for light touch and fine motor control

Steeve Bourane[1], **Katja S. Grossmann**[1], **Olivier Britz**[1], **Antoine Dalet**[1], **Marta Garcia Del Barrio**[1], **Floor J. Stam**[1], **Lidia Garcia-Campmany**[1], **Stephanie Koch**[1], and **Martyn Goulding**[1]

[1]Molecular Neurobiology Laboratory, The Salk Institute for Biological Studies, 10010 North Torrey Pines Road, La Jolla, CA 92037, USA

Abstract

Sensory circuits in the dorsal spinal cord integrate and transmit multiple cutaneous sensory modalities including the sense of light touch. Here we identify a population of excitatory interneurons (INs) in the dorsal horn that are important for transmitting innocuous light touch sensation. These neurons express the ROR alpha (RORα) nuclear orphan receptor and are selectively innervated by cutaneous low threshold mechanoreceptors (LTMs). Targeted removal of RORα INs in the dorsal spinal cord leads a marked reduction in behavioral responsiveness to light touch without affecting responses to noxious and itch stimuli. RORα IN-deficient mice also display a selective deficit in corrective foot movements. This phenotype, together with our demonstration that the RORα INs are innervated by corticospinal and vestibulospinal projection neurons, argues that the RORα INs direct corrective reflex movements by integrating touch information with descending motor commands from the cortex and cerebellum.

Keywords

mechanosensation; light touch; sensory coding; sensorimotor integration; motor control

INTRODUCTION

Animals use the sense of touch to identify and discriminate nearby objects, direct motor movements, and reinforce social interactions via affective touch (Abraira and Ginty, 2013; McGlone and Reilly, 2010; Rossignol et al., 2006). Specialized LTMs in the skin detect a

Correspondence to M.G Telephone: +1 858 453 4100 x1558; Fax: +1 858 450 2172 goulding@salk.edu.

SUPPLEMENTAL INFORMATION

Supplemental Information includes Expanded Experimental Procedures and six supplemental figures, Figures S1–S6.

AUTHOR CONTRIBUTIONS

SB, KSG, SK and MGDB characterized the RORα INs and performed the behavioral analyses. AD performed the electrophysiological recordings. OB, FJS and LGC generated the mice and contributed to the experimental analysis. SB and MG wrote the manuscript. MG supervised the study.

variety of touch modalities (Delmas et al., 2011; Li et al., 2011; Vrontou et al., 2013). Skin deformation and vibration are detected by rapidly adapting LTMs that innervate Meissner and Pacinian corpuscles, respectively, while slowly adapting Merkel cells and Ruffini organs respond to indentation and stretch (Delmas et al., 2011; McGlone and Reilly, 2010). C-LTMs and Aβ/Aδ lanceolate LTMs in hairy skin monitor the dynamic and static displacement of hair. Our knowledge of how specific somatosensory modalities, including touch, are relayed and gated within the dorsal spinal cord is more limited, in part because the functional studies undertaken so far have primarily employed genetic mutations that alter a broad swath of neurons (Cheng et al., 2004; Gross et al., 2002; Muller et al., 2002; Wang et al., 2013; Xu et al., 2013). Moreover, it is still unclear how cutaneous touch pathways intersect with descending motor pathways to control movement and posture.

The peripheral pathways that transmit thermoceptive, nociceptive, innocuous mechanosensory and proprioceptive stimuli are highly segregated (Basbaum et al., 2009; Lallemend and Ernfors, 2012). Unmyelinated C-nociceptors and lightly myelinated Aδ afferents that relay nociceptive, thermoceptive and pruritoceptive stimuli project to laminae I/II of the dorsal horn (Lallemend and Ernfors, 2012; Todd, 2010), while large diameter fast conducting neurons that carry proprioceptive information innervate neurons in the intermediate and ventral spinal cord (Jankowska, 1992; Lallemend and Ernfors, 2012). Innocuous touch modalities are transmitted by myelinated A-LTMs and unmyelinated C-LTMs that converge on laminae IIi-IV (Abraira and Ginty, 2013; Delmas et al., 2011; Lallemend and Ernfors, 2012; Lechner and Lewin, 2013). These and other findings argue that somatosensory information is encoded in the periphery by labeled lines of transmission. However, the extent to which these labeled lines extend into the central nervous system remains to be determined. It is known that cutaneous LTMs project and arborize within the dorsal horn in a modality-specific manner (Brown, 1981; Fyffe, 1992; Light and Perl, 1979a, b; Shortland and Woolf, 1993; Woolf, 1987). Hair follicle afferents terminate in lamina IIi and III (Woodbury et al., 2001). Meissner and Merkel cell afferents innervate lamina III and IV (Brown, 1981; Woolf, 1987), while the arbors of Pacinian corpuscle afferents localize to lamina III/dorsal lamina IV and lamina V (Brown, 1981; Semba et al., 1984). Finally, Ruffini organ afferents form collaterals in lamina III and have processes that extend into laminae IV/V (Brown, 1981). This anatomical organization suggests that defined mechanosensory modalities may be transmitted and processed by discrete IN cell types in the spinal cord.

In this study, we show that a class of dorsal spinal cord INs expressing the RORα nuclear orphan receptor are required for proper light touch perception. Ablating RORα INs in the caudal spinal cord markedly reduces the behavioral responses mice display to light touch, but not to noxious or itch stimuli. Mice lacking RORα INs also show a marked increase in footfalls and slips during beam walking, indicating the RORα INs are necessary for corrective foot movements and fine motor control. This motor deficit, in combination with neuronal tracing experiments showing the RORα INs are innervated by projection neurons in the lateral vestibular nucleus (LVN) and motor cortex, reveals a role for the RORα INs in integrating sensory inputs from cutaneous LTMs with descending motor signals from the cortex and vestibular system. In so doing, it provides evidence that the RORα INs function

as an important interneuronal node for coordinating descending motor commands with cutaneous mechanosensory feedback.

RESULTS

RORα identifies a distinct population of excitatory neurons in laminae IIi/III of the spinal cord

The neurons in the spinal cord that express RORα are primarily restricted to laminae IIi/III (Del Barrio et al., 2013). In mice carrying both the *ROR*α^{Cre} allele (Chou et al., 2013) and *Tau*$^{LSL\text{-}nlslacZ}$ reporter allele (Britz et al., 2014), β-galactosidase (β-gal) expression was localized to two bilateral columns of neurons in the dorsal horn (Figure 1A–C). Most importantly, β-gal was markedly absent from sensory neurons in the dorsal root ganglia (DRG) (Figure 1C). Transverse sections through the spinal cord showed that the RORα INs are largely restricted to laminae IIi/III, with the intermediate and ventral spinal cord being completely devoid of RORα expression (Figure 1C and Figure S1A).

To confirm that Cre recombination faithfully recapitulates RORα expression, P10 *ROR*α^{Cre}; *R26*$^{LSL\text{-}tdTomato}$ spinal cords were stained with antibodies to DsRed (tdTomato), RORα and NeuN (Figure 1D). 94.2±1.3% of the RORα$^+$/NeuN$^+$ neurons in lamina IIi/III expressed tdTomato. Conversely, 91.8±2.9% of the tdTomato$^+$/NeuN$^+$ neurons expressed RORα. Scattered non-neuronal NeuN-negative tdTomato$^+$ cells were present outside of lamina IIi/III (Figure 1D, asterisk). These cells are predominantly endothelial cells, but also include some glial cells. Anatomical analysis revealed that most RORα INs possess a radial, vertical or central cell-like morphologies (Figure 1G), and have dendritic fields that are largely confined to laminae IIi/III and dorsal lamina IV (Figure 1E–F and Figure S1B and C).

In keeping with their morphology, 86.1±2.7% of the RORα-Tomato$^+$ INs expressed Lmx1b (Figure 2A and E), which marks glutamatergic INs in the dorsal horn (Gross et al., 2002; Muller et al., 2002). By contrast, very few RORα-tdTomato$^+$ INs (1.2±0.5%) expressed the inhibitory marker Pax2 (Figure 2B and E). Further comparison of tdTomato and vesicular glutamate transporter *vGluT2* expression confirmed that the RORα$^+$ INs are primarily glutamatergic, with 91.6±0.4% coexpressing *vGluT2* (Figure 2C and E, Figure S2A–C). Moreover, a large fraction of them coexpressed cholecystokinin (Figure S2F), which is restricted to excitatory neurons in the dorsal horn (Hu et al., 2012; Xu et al., 2013). By contrast, only 3.1±0.9% of the RORα INs in *Gad1-GFP* mice expressed GFP (Figure 2D and E). Further analysis revealed two major molecular subsets of RORα INs: a dorsal population that colocalizes with PKCγ (Figure S2D and F) in lamina II inner, and a more ventral population of MafA$^+$/c-Maf$^+$/RORα$^+$ cells that are restricted to lamina III (Figure S2E and F)

Innervation of RORα INs by mechanosensory neurons

In view of their location in laminae IIi/III, we set out to determine if the RORα INs receive afferent input from innocuous mechanosensory neurons. CGRP and IB4 staining was used to compare the location of the RORα INs with the termination zones of peptidergic and non-peptidergic nociceptive afferents (Todd, 2010). The cell bodies of RORα INs were located

beneath the CGRP$^+$ and IB4$^+$ afferents in lamina I/II and II, respectively (Figure S3A). Only rarely did we detect putative contacts from nociceptive afferents onto RORα INs, indicating the RORα INs receive very little nociceptive input. By contrast, when a c-Ret-CFP transgene (Uesaka et al., 2008), was used to trace the central processes of mechanosensory afferents, we identified numerous CFP$^+$/vGluT1$^+$ synaptic contacts onto RORα INs (Figure S3B). These findings provide evidence that the RORα INs are innervated by cutaneous LTMs as opposed to cutaneous nociceptors.

Monosynaptic retrograde tracing using a pseudotyped EnvA-SADΔG-mCherry rabies virus (Wickersham et al., 2007) was employed to identify the sensory neuron cell types that innervate spinal RORα INs. These experiments were performed using an intersectional reporter (Li et al., 2013; Stam et al., 2012) that in combination with *ROR*α^{Cre} and *Cdx2::FlpO* restricts rabies virus entry to RORα INs in the caudal spinal cord (Figure 3A–C). Sensory neurons are not directly infected due to their lack of RORα expression. Injection of EnvA-SADΔG-mCherry rabies virus into the spinal cords of P5 *ROR*α^{Cre}; *Cdx2::FlpO*; *R26*$^{ds\text{-}HTB}$ mice, resulted in mCherry expression in multiple cutaneous LTM cell types, including cells with the following expression profiles: c-Ret$^+$/IB4$^-$ Aβ-LTMs (Figure 3D and K; 24.7±23%), TrkC$^+$/parvalbumin$^-$ Aβ-LTMs (Figure 3E and K, 22.0±2,5%) and TrkB$^+$ Aδ-LTMs (Figure 3F and K, 20.3±2.3%). Very few IB4$^+$ non-peptidergic nociceptors (Figure 3D and K, 0.66±0.33%) and parvalbumin$^+$ proprioceptors (Figure 3E and K, 3.1±1.9%). were labeled, demonstrating the RORα INs are primarily innervated by LTM afferents. We also identified a population of presynaptic neurons that express CGRP and NF200 (Figure 3K and S3G), which are likely to be a subtype of mechanoreceptor (Lawson et al., 2002). Our failure to detect mCherry-labeled Tyrosine Hydroxylase$^+$ C-LTM neurons (Figure 3G, (Li et al., 2011)) indicates that Aβ-LTMs and Aδ-LTMs, rather than C-LTMs, are the primary source of mechanosensory input to the RORα INs.

Our observation that rabies-derived mCherry labels the distal processes of sensory neurons allowed us to unambiguously identify the mechanosensory neuron cell types that innervate the RORα INs. mCherry$^+$/NF200$^+$ Aβ afferent fibers were present in the dermal papillae of glabrous skin where Meissner corpuscles are located (Figure 3H). This is consistent with mCherry-rabies labeling of calbindin$^+$ DRG afferents that innervate Meissner corpuscles (Figure S3E). Calretinin$^+$ DRG neurons and their associated Pacinian corpuscle nerve endings did not express mCherry (Figure S3C and D), indicating the RORα cells are not innervated by Pacinian LTMs. In hairy skin, we observed mCherry-labeled afferents innervating Merkel cells (Figure 3I). Aδ D-hair terminals (Figure 3J) and transverse lanceolate endings (Figure S3H) were also retrogradely labeled. The morphologies of the hairy skin LTMs labeled by rabies virus are consistent with the expression profile of mCherry in DRG neurons, as D-hair and lanceolate neurons express a combination of c-Ret, TrkB or TrkC (Lallemend and Ernfors, 2012). mCherry$^+$ afferents were occasionally seen together with Ruffini organ endings in the foot muscles (Figure S3F), although the exact extent of RORα IN innervation by Ruffini LTMs remains to be determined.

RORα INs are innervated by A-fiber afferents and are selectively activated by light touch

Whole cell recordings from RORα INs in lamina III revealed a spectrum of excitatory potentials that closely match the profile of presynaptic connections seen in the rabies tracing experiments. Short latency-low threshold potentials (<7 ms) with no failures and low jitter were detected in 11 of 31 cells following dorsal root stimulation (Figure 4A). These potentials most likely represent monosynaptic Aβ fibers, as Ia muscle spindle afferents do not terminate in lamina III (Brown, 1981; Jankowska, 1992). Low to intermediate threshold potentials that are likely to be either monosynaptic Aδ or A polysynaptic inputs were detected in another 12 cells (Figure 4C). 6 cells displayed long latency-high threshold potentials (>25 ms) that are characteristic of polysynaptic C-fiber inputs. Interestingly, 2 of these cells possessed an additional short latency-low threshold input, indicating some RORα INs receive a combination of myelinated A and unmyelinated C fiber innervation (Figure 4B). The exact nature of this polysynaptic C fiber innervation remains to be determined, although it may be derived from C-LTMs that sense pleasant touch (Liu et al., 2007; Vrontou et al., 2013).

We then asked if light brush stimulation activates the immediate early gene c-Fos in RORα INs. Light brushing of the plantar (underside) surface of the foot (Figure 4D–F and J), and the hairy skin of the lower limb (Figure 4J), resulted in extensive expression of c-Fos in lamina IIi/III RORα INs. By contrast, injection of capsaicin into the foot resulted in very little c-Fos induction in RORα INs (3.1±0.9%; Figure 4G–I and J). Instead, c-Fos induction was largely restricted to laminae I/II and lamina V. Some activation of c-Fos was also observed in lamina I/II neurons in response to brushing (Figure 4D). This may reflect sensitization due to the prolonged brush stimulation needed for c-Fos induction in lamina IIi/III neurons, or it might be due to the activation of nociceptive pathways by innocuous touch at early postnatal stages (Koch et al., 2012).

Ablating RORα INs in the dorsal spinal cord impairs light touch

To determine the functional contribution RORα INs make to somatosensation, we employed a recently developed intersectional *Tau*$^{\text{ds-DTR}}$ allele (Figure 5A; (Britz et al., 2014)) to inducibly ablate the RORα INs in the adult spinal cord. When used in combination with *ROR*α$^{\text{Cre}}$ and a *Cdx2::FlpO* transgene, which is only expressed in caudal regions of the mouse (Britz et al., 2014), we were able to selectively target diphtheria toxin receptor (DTR) expression to RORα INs in the caudal spinal cord. RORα-expressing cells in the anterior CNS and in non-neuronal tissues were not affected by diphtheria toxin (DTX) treatment (Figure 5B and C). Using a *R26*$^{\text{LSL-tdTomato}}$ reporter to trace the RORα cells, we estimate that >95% of the RORα INs in the lumbar cord were ablated by DTX treatment (Figure 5D–F). Cell killing was largely restricted to excitatory Lmx1b^{+} INs in lamina IIi/III (Figure5E and 5G), where RORα and Lmx1b are coexpressed, with the number of inhibitory Pax2^{+} neurons in the dorsal horn remaining unchanged (Figure 5H).

To confirm cell ablation is restricted to RORα INs, we analyzed the expression of several excitatory dorsal horn markers (Brohl et al., 2008; Del Barrio et al., 2013; Gross et al., 2002; Muller et al., 2002). As expected, there was a corresponding reduction in the number of cells expressing PKCβ, MafA, c-Maf, and calbindin (Figure S4A–D), while excitatory calretinin^{+}

INs that do not express RORα and GAD1$^+$ inhibitory INs were unaffected (Figure S4E and F). We also verified that RORα IN ablation does not alter the lamina organization of sensory afferent terminals in dorsal spinal cord. CGRP$^+$ and IB4$^+$ nociceptive terminals projected normally to laminae I/II (Figure S4G and H) and there was no gross change in the central projections of vGluT1$^+$ mechanosensory afferents (Figure S4I–J). The termination patterns of peripheral nerve endings (Figure S4K–L) were also unchanged following RORα IN-ablation demonstrating that the loss of these cells does not cause any major change in central and peripheral sensory innervation.

RORα IN-ablated mice were then subjected to a battery of sensory tests. Strikingly, mice lacking spinal RORα INs displayed a specific sensory impairment in dynamic and static light touch. In particular, the response to light brushing on the plantar surface of the foot was markedly diminished as compared to control littermates (Figure 5I; 30±7.9% versus 76±6.5% of trials). Furthermore, the latency to detecting a piece of sticky tape on the plantar surface of the foot was also increased 2.5 fold (Figure 5J; control 78.9±17.7 secs versus RORα IN-ablated 192.9±20.4 secs), thereby demonstrating a substantial reduction in responsiveness to static touch. We also observed a marked reduction in tactile sensation on the hairy skin of mice lacking RORα INs (Figure 5K) indicating the RORα INs contribute to light touch perception in hairy skin. By contrast, RORα IN deficient mice displayed no change in their responses to mechanical pain (Figure 5L–N) or sensitivity to heat and cold (Figure 5O and P). Responses to chemically-induced itch were also unchanged (Figure 5Q and R). Finally, there was no difference in acute pain sensation following the injection of capsaicin and formalin (Figure 5S and T). In summary, depleting RORα INs from the dorsal spinal cord results in the selective loss of light touch without altering responsiveness to mechanical, thermal and chemical pain, and to chemical itch.

RORα IN-ablated mice display deficits in corrective motor movements

Our ability to genetically manipulate the RORα IN population led us examine the contribution that the RORα INs make to motor control in mice (Figure 6). Gross behavioral analyses failed to uncover any pronounced change in locomotor activity in RORα IN-ablated mice (Figure S5), with most measures of locomotor function being largely normal. There was no difference between control and RORα IN-ablated mice in total distance traveled, vertical activity or total number of jumps performed during open-field testing (Figure S5A–C). Muscle strength, as assessed by the hanging wire test, was also normal in the RORα IN-ablated mice (Figure S5D). There was also no marked change in gross motor coordination as assessed by the accelerating rotarod and limb coordination during treadmill and ladder beam walking (Figure S5E–I).

By contrast, when the raised beam test was used to assess fine motor control during locomotion, a significant increase hindlimb missteps and footfalls was seen in RORα IN-ablated mice traversing a 5 mm beam as compared to control mice (Figure 6A–C (3.73±0.73 episodes per crossing for RORα IN-ablated mice versus 1.29±0.3 episodes per crossing for control mice)). Most notably, this increase in missteps/footfalls was restricted to the hindlimbs, which is consistent with the depletion of RORα INs at hindlimb levels but not at forelimb levels. In sum, our results demonstrate that RORα IN-mediated feedback to the

motor system is essential for corrective movements, while being largely dispensable for gross motor movements.

RORα INs form synaptic contacts with motor neurons and premotor neurons

To further probe the nature of the RORα IN motor phenotype, we asked if the RORα INs provide excitatory inputs to motor neurons and molecularly-identified premotor IN cell types that control locomotion in mice (Arber, 2012; Goulding, 2009; Grillner and Jessell, 2009; Kiehn, 2011). To visualize the terminal processes of RORα INs, *RORα*^{Cre} mice were crossed with conditional *Thy1*$^{LSL\text{-}YFP}$ reporter mice (Buffelli et al., 2003). We observed multiple YFP$^+$/vGluT2$^+$ contacts on motor neurons in the lumbar lateral motor column (Figure 6D). These vGluT2$^+$ contacts are likely to be functional synapses as we find mCherry-positive premotor RORα INs in the lumbar spinal cords of *RORα*^{Cre}; *Tau*$^{LSL\text{-}lacZ}$ mice following injection of pseudotyped SADΔG-mCherry rabies virus and AAV-G into the gastrocnemius (ankle extensor) and tibialis anterior (ankle flexor) muscles (Figure 6E–G). We also looked for YFP$^+$/vGluT2$^+$ contacts on lamina X V0c cholinergic neurons (Stepien et al., 2010; Zagoraiou et al., 2009), which are the source of muscarinic cholinergic inputs to motor neurons (Miles et al., 2007). RORα IN-derived contacts were observed on the soma of these cells (Figure 6H), suggesting the RORα INs are a source of excitatory drive to the V0c IN population. DsRed$^+$/vGluT2$^+$ bouton-like contacts were also found on CFP$^+$ V2a INs in *RORα*^{Cre}; *R26*$^{LSL\text{-}tdTomato}$; *Chx10*^{CFP} mice indicating putative synaptic connections between RORα INs and Chx10$^+$ V2a INs (Figure 6I). These analyses are likely to substantially underestimate the number of putative RORα IN-derived synaptic contacts on premotor and motor neurons, given that excitatory contacts are most abundant on dendrites, Taken together, these tracing studies provide evidence that excitatory RORα INs relay touch information from cutaneous LTMs to the spinal motor system.

In view of the contribution that the corticospinal tract (CST) and lateral vestibulospinal tract (LVST) pathways make to fine motor control and balance (Armstrong, 1988; Ito, 2012), we asked whether CST neurons and LVST neurons synapse directly onto the RORα INs in the lumbar spinal cord. Targeted infection of lumbar level RORα INs with EnvA-SADΔG-mCherry rabies virus resulted in monosynaptic rabies virus labeling of LVST neurons in the lateral vestibular nucleus (Figure 7A). These cells, which are innervated by calbindin$^+$ Purkinje cells (Figure 7A, inset, arrows), constitute a major vestibular efferent pathway from the cerebellum to the spinal cord (Ito, 2012). We also found multiple mCherry-labeled neurons (Figure 7B) in lamina V of the contralateral mouse primary motor cortex that had the typical pyramidal morphology of corticospinal projection neurons (Figure 7B and C). When whole cell recordings were performed on RORα INs in the lumbar cord (L4), 8 of 10 RORα INs displayed monosynaptic excitatory potentials in response to stimulating A fiber sensory afferents and the ventral dorsal funiculus that contains the axons of corticospinal projection neurons (Figure 7D–F). This protocol has been shown to selectively activate descending corticospinal axons (Hantman and Jessell, 2010), however, some synaptic potentials might arise from the antidromic stimulation of ascending dorsal column axons. Additional evidence for the presence of convergent corticospinal and sensory inputs onto the RORα INs comes from anatomical studies showing lumbar RORα INs are decorated with PKCγ$^+$/vGluT1$^+$ and Emx1-GFP$^+$/vGluT1$^+$ contacts from corticospinal projection neurons

(Figure 7G and H). These same cells are also contacted by vGluT1$^+$ processes, which are likely to be derived from mechanosensory afferents (Figure 7G and H, arrowheads).

DISCUSSION

This study identifies a specific class of neurons in the dorsal spinal cord that have an essential role in sensing light touch. The RORα INs transmit innocuous mechanical stimuli from both the hairy and glabrous skin, and depleting the spinal cord of RORα INs leads to a selective mechanosensory deficit that closely matches the repertoire of inputs these cells receive from cutaneous LTMs. We propose that the RORα INs serve as an integrative node that merges sensory input from cutaneous LTMs with descending signals from the cortex and cerebellum to generate the postural adjustments and corrective foot movements that are used to counteract foot slippage.

Coding of mechanical stimuli by RORα INs

Our results showing discriminative light touch behaviors are impaired in RORα IN-ablated mice (Figure 5I and J), whereas nocifensive behaviors are not (Figure 5), provides evidence that somatosensory inputs to the spinal cord are processed and transmitted in a modality-specific manner. This finding, together with studies showing excitatory neurons located dorsal to the RORα INs in lamina II transmit mechanical pain (Duan et al., 2014), is consistent with the existence of 'labeled' interneuronal lines of transmission with the CNS, and it supports a model in which innocuous versus noxious touch modalities are routed through different interneuronal pathways in the spinal cord. We propose that light touch is gated by RORα INs in lamina IIi/III, whereas mechanical pain is processed by somatostatin$^+$ neurons in lamina II, which is in accordance with the general organization of nociceptive and mechanosensory projections in the dorsal spinal cord (Abraira and Ginty, 2013; Lechner and Lewin, 2013; Todd, 2010).

The RORα INs are innervated by multiple LTM subtypes (Figure 3 and Figure S3), arguing that they process multiple streams of mechanosensory input from the skin. In the trigeminal vibrissa system, tactile inputs converge on projection neurons that receive tactile information from slowly-adapting Merkel cell afferents and from rapidly-adapting lanceolate afferents (Sakurai et al., 2013). The RORα INs differ from these projection neurons in that they are exclusively local circuit neurons (Figure 1 and Figure S1). The majority of RORα INs appear to be innervated by a single sensory afferent fiber type, with 29 of 31 recorded cells displaying a single depolarizing potential following dorsal root stimulation (Figure 4). Although this finding is consistent with innervation by a single mechanosensory cell type, we cannot exclude the possibility that individual RORα INs receive more than one type of mechanosensory input. For example, dual depolarizing potentials consistent with monosynaptic A and polysynaptic C inputs were detected in two RORα cells (Figure 4B), raising the possibility that some RORα cells merge sensory information from A-LTMs and C-LTMs.

Our observation that the RORα INs are molecularly and anatomically heterogeneous (Figure S1 and S2), suggests that subpopulations of RORα INs may process different types of mechanosensory information. Different LTM cell types are known to innervate discrete

laminar territories in the dorsal horn (Li et al., 2011; Schouenborg, 2008), raising the possibility that different forms of touch, e.g. caress or pressure, activate different combinations of RORα IN subtypes. For instance, PKCγ^{+}/RORα^{+} INs in lamina IIi are likely to be innervated by Aδ afferents (Li et al., 2011; Light and Perl, 1979a, b; Todd, 2010), while RORα^{+}/MafA^{+}/c-Maf^{+} neurons in lamina III would be activated by Aβ-LTM inputs. Sensory coding by the RORα INs may therefore play an important role in discriminating different forms of touch.

One question that arises from this study is whether innocuous touch is mediated solely by the RORα INs or whether other excitatory IN cell types in the dorsal horn also contribute to the sense of light touch? The deficits in sensing light touch the RORα IN-ablated mice are very pronounced in the glabrous skin, arguing that light touch information from the glabrous skin is primarily gated via RORα INs. However, it is likely that other excitatory INs contribute to innocuous touch transmission from hairy skin, as RORα INs are not directly innervated by TH^{+} C-LTMs (Figure 3). RORα INs also lack inputs from Pacinian corpuscles (Figure S3), with the MafA^{+}/c-Maf^{+} neurons in lamina IV that lack RORα expression being the most likely candidates for processing information from Pacinian LTMs.

RORα INs: a nexus for integrating cutaneous touch and descending motor control signals

Human studies have shown that the cutaneous sensory, visual and vestibular systems all contribute to fine motor control and balance (Perry et al., 2000; Stal et al., 2003). It has also been shown in cats, that the corticospinal pathway displays functional convergence on cutaneous reflex pathways (Bretzner and Drew, 2005; Lundberg and Voorhoeve, 1962). What was not clear was how information from these different pathways is merged to provide a coherent set of commands to the spinal motor system. Our discovery that RORα INs are innervated by descending motor pathways from the cortex and cerebellum suggest that much of this integration may occur at the level of the dorsal horn with the RORα INs playing a prominent role in integrating cutaneous sensory information with descending motor commands. We propose that the RORα INs, via their direct excitatory inputs to premotor neurons and motor neurons, function as the core integrative element of a sensorimotor circuit for corrective motor behaviors and fine motor control (Figure 7I).

Mechanosensory feedback from the sole of the foot makes a major contribution to postural stability (Perry et al., 2000; Stal et al., 2003), with these pathways often being compromised in elderly and Parkinson’s patients that are prone to falling (Patel et al., 2009; Pratorius et al., 2003; Zia et al., 2003). With respect to the motor phenotype in mice lacking RORα INs, the loss of sensory feedback from Meissner corpuscles in the sole of the foot that are used to sense slippage would contribute to the increase in foot slips, and possible issues with balance, during beam walking. Deficits in detecting skin deformation and edges due to impaired signaling from Merkel cells and Ruffini endings may also be a factor. The RORα INs are innervated by LVST neurons, which points to an important role for the RORα INs in gating the output of LVN to the spinal cord. LVST neurons functionally facilitate limb extension (Grillner et al., 1971; Hultborn et al., 1976), in part via their excitatory actions on Ia reciprocal inhibitory neurons. Our observation that a subpopulation of V2b INs possess

the features of Ia reciprocal inhibitory neurons (Zhang et al., 2014), coupled with rabies-tracing experiments showing the RORα INs synapse onto V2b INs (FS and MG; unpublished data), raises the possibility that the vestibular control of limb extension may be partly mediated by the excitatory actions of RORα INs on V2b-derived Ia reciprocal inhibitory neurons that inhibit flexor motor neurons.

RORα IN-dependent sensory feedback is largely dispensable for gross locomotor movements. This finding concurs with studies in the cat showing gross locomotor behaviors such as walking are largely independent of cutaneous feedback (Rossignol et al., 2006). Nonetheless, light touch can exert strong phase-dependent effects on locomotion, as exemplified by the stumbling corrective response and paw shake reflex (Forssberg, 1979; Quevedo et al., 2005; Rossignol et al., 2006) with the RORα INs being potential candidates for mediating these corrective reflexes. The limited role that light touch plays in shaping coarse stepping movements suggests the sensorimotor system is functionally organized so that light touch is primarily used for corrective motor movements. In this way, vestibulospinal, rubrospinal and corticospinal pathways that intersect with cutaneous sensory pathways in the dorsal spinal cord have the capacity to elicit dynamic changes in posture and limb/foot/digit position without disrupting the overall locomotor pattern. Under certain conditions, however, these pathways can alter the locomotor pattern.

Sensorimotor circuits in the spinal cord and cerebellum are organized into action-based sensorimotor modules that constitute a functional scaffold for corrective and/or reflexive motor behaviors (Schouenborg, 2008). We propose that the RORα IN touch circuit represents an action-based sensorimotor circuit for corrective motor behaviors. Specifically, the RORα INs couple a tactile map of the body surface to motor pathways via their connections to elements of the spinal motor circuitry (Figure 6) and to postsynaptic dorsal column (PSDC) projection neurons (Figure S6) that relay tactile sensory information to the cerebellum (Ito, 2012). In this context, the RORα IN-PSDC-cerebellar pathway would operate as an error detection system to correct motor movements in response to tactile sensory feedback (Apps and Garwicz, 2005). In summary, the RORα IN-PSDC-cerebellum pathway and the reciprocal LVST-RORα IN pathway constitute a spinocerebellar feedback loop that utilizes cutaneous sensorimotor feedback to shape the fine corrective movements animals use for dynamic motor control.

EXPERIMENTAL PROCEDURES

Mouse Lines

Multiple mouse lines were used for this study. Mice were maintained on a mixed background and littermates were used as controls for all experiments. *ROR*α^{Cre} mice were kindly provided by Dr. Dennis O'Leary (Chou et al., 2013). Littermates lacking the *Cdx2::FlpO* allele were used as controls for all behavioral experiments. Expression analyses were performed using the *R26*$^{LSL\text{-}tdTomato}$ (Madisen et al., 2010), *Tau*$^{LSL\text{-}nlslacZ}$ (Britz et al., 2014) and *R26*$^{ds\text{-}HTB}$ mice (Stam et al., 2012). *R26*$^{ds\text{-}HTB}$ mice *R26*$^{LSL\text{-}TVA}$ mice (Seidler et al., 2008) were used for transsynaptic tracing and morphological analysis with EnvA-pseudotyped rabies virus. The *Tau*$^{ds\text{-}DTR}$ *and Cdx2::FlpO* mouse lines (Britz et al., 2014) were used for the behavioral analyses.

Immunohistochemistry

Immunohistochemical analyses were performed on cryostat sections of fixed tissues using previously described methods (Bourane et al., 2007; Gross et al., 2002).

In situ hybridization

In situ hybridization was performed as previously described (Bourane et al., 2007).

c-Fos Induction

P6 *ROR*α^{Cre}; *R26*$^{ds\text{-}HTB}$ mice, restrained in a specially designed enclosure, were acclimated for 10 min prior to stimulation. For light brush stimulation, a soft paint brush was used to gently stroke the plantar surface (glabrous) or dorsal surface (hairy) of the hindpaw for 45 min at approximately 0.5 Hz. To activate pain pathways, 6 μl of capsaicin (1 mg in 10 ml saline, 7% Tween-80) was injected subcutaneously into the plantar surface of the hindpaw. A 60 min chase time was included between stimulation and sacrificing the animals. Spinal cords were immediately dissected and fixed in 4% paraformaldehyde/PBS. Frozen sections from the lumbar spinal cord were immunostained with antibodies specific for c-Fos and β-galactosidase.

Rabies Virus Tracing

Injections of pseudotyped rabies virus into the lumbar spinal cord of P14 *ROR*α^{Cre}; *R26*$^{LSL\text{-}TVA}$ mice were used to examine RORα IN morphology For transsynaptic tracing studies, injections were made into the lumbar cord of *ROR*α^{Cre}; *Cdx2::FlpO; R26*$^{ds\text{-}HTB}$ animals at P5 or P10. For muscle injections, single muscles were injected with G protein-deleted-mCherry rabies virus according to (Stepien et al., 2010).

Behavioral Testing and Analysis

All the behavioral tests were performed blind to the genotype of the animals. Animal experiments were conducted according to NIH guidelines using protocols approved by the Salk Institute for Biological Studies IACUC. Detailed protocols for all behavioral tests are described in Expanded Experimental Procedures.

Electrophysiology

Whole cell recordings and dorsal root stimulation were performed using sagittal hemicords prepared from postnatal P5-P21 *ROR*α^{Cre}; *Thy1*$^{LSL\text{-}YFP}$ mice as described by (Torsney and MacDermott, 2006), with minor modifications. The CST was stimulated with a concentric bipolar electrode (FHC) positioned 3–4 mm rostral to the recorded neuron. Stimulation was performed at 2Hz (100μA, 0.1ms) to exclude retrograde axonal transmission. See Extended Experimental Procedures.

Quantitative Analysis and Statistics

Cell counts were determined by analyzing 3–6 spinal cords (5–10 sections each) per genotype. All data are presented as the mean ± standard error of the mean (SEM) with n indicating the number of mice analyzed. Statistical analyses were performed by two-tailed, unpaired Student's *t* test. p values below 0.05 were considered to be statistically significant.

Supplementary Material

Refer to Web version on PubMed Central for supplementary material.

ACKNOWLEDGEMENTS

We thank Chris Kintner, Qiufu Ma, John Thomas for discussions and helpful comments on this study. We acknowledge Bo Duan for advice on behavioral tests and Catherine Farrokhi for help with the rotarod and open field analysis. This work was supported by the National Institutes of Health (NS080586, NS086372, P01 NS072031) to MG, the Caterina Foundation to SB and the Humboldt Foundation to KSG.

REFERENCES

Abraira VE, Ginty DD. The sensory neurons of touch. Neuron. 2013; 79:618–639. [PubMed: 23972592]

Apps R, Garwicz M. Anatomical and physiological foundations of cerebellar information processing. Nature reviews Neuroscience. 2005; 6:297–311.

Arber S. Motor circuits in action: specification, connectivity, and function. Neuron. 2012; 74:975–989. [PubMed: 22726829]

Armstrong DM. The supraspinal control of mammalian locomotion. J Physiol. 1988; 405:1–37. [PubMed: 3076600]

Basbaum AI, Bautista DM, Scherrer G, Julius D. Cellular and molecular mechanisms of pain. Cell. 2009; 139:267–284. [PubMed: 19837031]

Bourane S, Mechaly I, Venteo S, Garces A, Fichard A, Valmier J, Carroll P. A SAGE-based screen for genes expressed in sub-populations of neurons in the mouse dorsal root ganglion. BMC Neurosci. 2007; 8:97. [PubMed: 18021428]

Bretzner F, Drew T. Motor cortical modulation of cutaneous reflex responses in the hindlimb of the intact cat. J Neurophysiol. 2005; 94:673–687. [PubMed: 15788517]

Britz OJZ, Grossmann KS, Dyck J, Kim JC, Dymecki S, Gosgnach S, Goulding M. A genetically-defined asymmetry underlies the inhibitory control of flexor-extensor locomotor movements. eLife (submitted). 2014

Brohl D, Strehle M, Wende H, Hori K, Bormuth I, Nave KA, Muller T, Birchmeier C. A transcriptional network coordinately determines transmitter and peptidergic fate in the dorsal spinal cord. Dev Biol. 2008; 322:381–393. [PubMed: 18721803]

Brown, AG. Organization in the spinal cord : the anatomy and physiology of identified neurones. Berlin; New York: Springer-Verlag; 1981.

Buffelli M, Burgess RW, Feng G, Lobe CG, Lichtman JW, Sanes JR. Genetic evidence that relative synaptic efficacy biases the outcome of synaptic competition. Nature. 2003; 424:430–434. [PubMed: 12879071]

Cheng L, Arata A, Mizuguchi R, Qian Y, Karunaratne A, Gray PA, Arata S, Shirasawa S, Bouchard M, Luo P, et al. Tlx3 and Tlx1 are post-mitotic selector genes determining glutamatergic over GABAergic cell fates. Nat Neurosci. 2004; 7:510–517. [PubMed: 15064766]

Chou SJ, Babot Z, Leingartner A, Studer M, Nakagawa Y, O'Leary DD. Geniculocortical input drives genetic distinctions between primary and higher-order visual areas. Science. 2013; 340:1239–1242. [PubMed: 23744949]

Del Barrio MG, Bourane S, Grossmann K, Schule R, Britsch S, O'Leary DD, Goulding M. A transcription factor code defines nine sensory interneuron subtypes in the mechanosensory area of the spinal cord. PLoS One. 2013; 8:e77928. [PubMed: 24223744]

Delmas P, Hao J, Rodat-Despoix L. Molecular mechanisms of mechanotransduction in mammalian sensory neurons. Nat Rev Neurosci. 2011; 12:139–153. [PubMed: 21304548]

Duan B, Cheng L, Bourane S, Britz O, Padilla C, Garcia-Campmany L, Krashes M, Knowlton W, Velasquez T, Ren X, et al. Identification of Spinal Circuits Transmitting and Gating Mechanical Pain. Cell. 2014; 159:1417–1432. [PubMed: 25467445]

Forssberg H. Stumbling corrective reaction: a phase-dependent compensatory reaction during locomotion. J Neurophysiol. 1979; 42:936–953. [PubMed: 479924]

Fyffe, REW. Laminar organization of primary afferent terminals in the mammalian spinal cord. Sensory Neurons: Diversity. Scott, SA., editor. New York: Development and Plasticity Oxford University Press; 1992. p. 131-139.

Goulding M. Circuits controlling vertebrate locomotion: moving in a new direction. Nat Rev Neurosci. 2009; 10:507–518. [PubMed: 19543221]

Grillner S, Hongo T, Lund S. Convergent effects on alpha motoneurones from the vestibulospinal tract and a pathway descending in the medial longitudinal fasciculus. Exp Brain Res. 1971; 12:457–479. [PubMed: 5093725]

Grillner S, Jessell TM. Measured motion: searching for simplicity in spinal locomotor networks. Curr Opin Neurobiol. 2009; 19:572–586. [PubMed: 19896834]

Gross MK, Dottori M, Goulding M. Lbx1 specifies somatosensory association interneurons in the dorsal spinal cord. Neuron. 2002; 34:535–549. [PubMed: 12062038]

Hantman AW, Jessell TM. Clarke's column neurons as the focus of a corticospinal corollary circuit. Nat Neurosci. 2010; 13:1233–1239. [PubMed: 20835249]

Hu J, Huang T, Li T, Guo Z, Cheng L. c-Maf is required for the development of dorsal horn laminae III/IV neurons and mechanoreceptive DRG axon projections. J Neurosci. 2012; 32:5362–5373. [PubMed: 22514301]

Hultborn H, Illert M, Santini M. Convergence on interneurones mediating the reciprocal Ia inhibition of motoneurones. III. Effects from supraspinal pathways. Acta Physiol Scand. 1976; 96:368–391. [PubMed: 179277]

Ito, M. The cerebellum : brain for an implicit self. Upper Saddle River, N.J.: FT Press; 2012.

Jankowska E. Interneuronal relay in spinal pathways from proprioceptors. Prog Neurobiol. 1992; 38:335–378. [PubMed: 1315446]

Kiehn O. Development and functional organization of spinal locomotor circuits. Curr Opin Neurobiol. 2011; 21:100–109. [PubMed: 20889331]

Koch SC, Tochiki KK, Hirschberg S, Fitzgerald M. C-fiber activity-dependent maturation of glycinergic inhibition in the spinal dorsal horn of the postnatal rat. Proc Natl Acad Sci U S A. 2012; 109:12201–12206. [PubMed: 22778407]

Lallemend F, Ernfors P. Molecular interactions underlying the specification of sensory neurons. Trends Neurosci. 2012; 35:373–381. [PubMed: 22516617]

Lawson SN, Crepps B, Perl ER. Calcitonin gene-related peptide immunoreactivity and afferent receptive properties of dorsal root ganglion neurones in guinea-pigs. J Physiol. 2002; 540:989–1002. [PubMed: 11986384]

Lechner SG, Lewin GR. Hairy sensation. Physiology (Bethesda). 2013; 28:142–150. [PubMed: 23636260]

Li L, Rutlin M, Abraira VE, Cassidy C, Kus L, Gong S, Jankowski MP, Luo W, Heintz N, Koerber HR, et al. The functional organization of cutaneous low-threshold mechanosensory neurons. Cell. 2011; 147:1615–1627. [PubMed: 22196735]

Light AR, Perl ER. Reexamination of the dorsal root projection to the spinal dorsal horn including observations on the differential termination of coarse and fine fibers. J Comp Neurol. 1979a; 186:117–131. [PubMed: 447880]

Light AR, Perl ER. Spinal termination of functionally identified primary afferent neurons with slowly conducting myelinated fibers. J Comp Neurol. 1979b; 186:133–150. [PubMed: 109477]

Liu Q, Vrontou S, Rice FL, Zylka MJ, Dong X, Anderson DJ. Molecular genetic visualization of a rare subset of unmyelinated sensory neurons that may detect gentle touch. Nat Neurosci. 2007; 10:946–948. [PubMed: 17618277]

Lundberg A, Voorhoeve P. Effects from the pyramidal tract on spinal reflex arcs. Acta Physiol Scand. 1962; 56:201–219. [PubMed: 13931674]

Madisen L, Zwingman TA, Sunkin SM, Oh SW, Zariwala HA, Gu H, Ng LL, Palmiter RD, Hawrylycz MJ, Jones AR, et al. A robust and high-throughput Cre reporting and characterization system for the whole mouse brain. Nat Neurosci. 2010; 13:133–140. [PubMed: 20023653]

McGlone F, Reilly D. The cutaneous sensory system. Neurosci Biobehav Rev. 2010; 34:148–159. [PubMed: 19712693]

Miles GB, Hartley R, Todd AJ, Brownstone RM. Spinal cholinergic interneurons regulate the excitability of motoneurons during locomotion. Proc Natl Acad Sci U S A. 2007; 104:2448–2453. [PubMed: 17287343]

Muller T, Brohmann H, Pierani A, Heppenstall PA, Lewin GR, Jessell TM, Birchmeier C. The homeodomain factor lbx1 distinguishes two major programs of neuronal differentiation in the dorsal spinal cord. Neuron. 2002; 34:551–562. [PubMed: 12062039]

Patel M, Magnusson M, Kristinsdottir E, Fransson PA. The contribution of mechanoreceptive sensation on stability and adaptation in the young and elderly. Eur J Appl Physiol. 2009; 105:167–173. [PubMed: 18925415]

Perry SD, McIlroy WE, Maki BE. The role of plantar cutaneous mechanoreceptors in the control of compensatory stepping reactions evoked by unpredictable, multi-directional perturbation. Brain Res. 2000; 877:401–406. [PubMed: 10986360]

Pratorius B, Kimmeskamp S, Milani TL. The sensitivity of the sole of the foot in patients with Morbus Parkinson. Neurosci Lett. 2003; 346:173–176. [PubMed: 12853112]

Quevedo J, Stecina K, Gosgnach S, McCrea DA. Stumbling corrective reaction during fictive locomotion in the cat. J Neurophysiol. 2005; 94:2045–2052. [PubMed: 15917325]

Rossignol S, Dubuc R, Gossard JP. Dynamic sensorimotor interactions in locomotion. Physiol Rev. 2006; 86:89–154. [PubMed: 16371596]

Sakurai K, Akiyama M, Cai B, Scott A, Han BX, Takatoh J, Sigrist M, Arber S, Wang F. The organization of submodality-specific touch afferent inputs in the vibrissa column. Cell Rep. 2013; 5:87–98. [PubMed: 24120861]

Schouenborg J. Action-based sensory encoding in spinal sensorimotor circuits. Brain Res Rev. 2008; 57:111–117. [PubMed: 17920132]

Seidler B, Schmidt A, Mayr U, Nakhai H, Schmid RM, Schneider G, Saur D. A Cre-loxP-based mouse model for conditional somatic gene expression and knockdown in vivo by using avian retroviral vectors. Proc Natl Acad Sci U S A. 2008; 105:10137–10142. [PubMed: 18621715]

Semba K, Masarachia P, Malamed S, Jacquin M, Harris S, Egger MD. Ultrastructure of pacinian corpuscle primary afferent terminals in the cat spinal cord. Brain Res. 1984; 302:135–150. [PubMed: 6203612]

Shortland P, Woolf CJ. Morphology and somatotopy of the central arborizations of rapidly adapting glabrous skin afferents in the rat lumbar spinal cord. J Comp Neurol. 1993; 329:491–511. [PubMed: 8454737]

Stal F, Fransson PA, Magnusson M, Karlberg M. Effects of hypothermic anesthesia of the feet on vibration-induced body sway and adaptation. J Vestib Res. 2003; 13:39–52. [PubMed: 14646023]

Stam FJ, Hendricks TJ, Zhang J, Geiman EJ, Francius C, Labosky PA, Clotman F, Goulding M. Renshaw cell interneuron specialization is controlled by a temporally restricted transcription factor program. Development. 2012; 139:179–190. [PubMed: 22115757]

Stepien AE, Tripodi M, Arber S. Monosynaptic rabies virus reveals premotor network organization and synaptic specificity of cholinergic partition cells. Neuron. 2010; 68:456–472. [PubMed: 21040847]

Todd AJ. Neuronal circuitry for pain processing in the dorsal horn. Nat Rev Neurosci. 2010; 11:823–836. [PubMed: 21068766]

Torsney C, MacDermott AB. Disinhibition opens the gate to pathological pain signaling in superficial neurokinin 1 receptor-expressing neurons in rat spinal cord. J Neurosci. 2006; 26:1833–1843. [PubMed: 16467532]

Uesaka T, Nagashimada M, Yonemura S, Enomoto H. Diminished Ret expression compromises neuronal survival in the colon and causes intestinal aganglionosis in mice. J Clin Invest. 2008; 118:1890–1898. [PubMed: 18414682]

Vrontou S, Wong AM, Rau KK, Koerber HR, Anderson DJ. Genetic identification of C fibres that detect massage-like stroking of hairy skin in vivo. Nature. 2013; 493:669–673. [PubMed: 23364746]

Wang X, Zhang J, Eberhart D, Urban R, Meda K, Solorzano C, Yamanaka H, Rice D, Basbaum AI. Excitatory superficial dorsal horn interneurons are functionally heterogeneous and required for the full behavioral expression of pain and itch. Neuron. 2013; 78:312–324. [PubMed: 23622066]

Wickersham IR, Lyon DC, Barnard RJ, Mori T, Finke S, Conzelmann KK, Young JA, Callaway EM. Monosynaptic restriction of transsynaptic tracing from single, genetically targeted neurons. Neuron. 2007; 53:639–647. [PubMed: 17329205]

Woodbury CJ, Ritter AM, Koerber HR. Central anatomy of individual rapidly adapting low-threshold mechanoreceptors innervating the "hairy" skin of newborn mice: early maturation of hair follicle afferents. J Comp Neurol. 2001; 436:304–323. [PubMed: 11438932]

Woolf CJ. Central terminations of cutaneous mechanoreceptive afferents in the rat lumbar spinal cord. J Comp Neurol. 1987; 261:105–119. [PubMed: 3624538]

Xu Y, Lopes C, Wende H, Guo Z, Cheng L, Birchmeier C, Ma Q. Ontogeny of excitatory spinal neurons processing distinct somatic sensory modalities. J Neurosci. 2013; 33:14738–14748. [PubMed: 24027274]

Zagoraiou L, Akay T, Martin JF, Brownstone RM, Jessell TM, Miles GB. A cluster of cholinergic premotor interneurons modulates mouse locomotor activity. Neuron. 2009; 64:645–662. [PubMed: 20005822]

Zhang J, Lanuza GM, Britz O, Wang Z, Siembab VC, Zhang Y, Velasquez T, Alvarez FJ, Frank E, Goulding M. V1 and V2b interneurons secure the alternating flexor-extensor motor activity mice require for limbed locomotion. Neuron. 2014; 82:138–150. [PubMed: 24698273]

Zia S, Cody FW, O'Boyle DJ. Discrimination of bilateral differences in the loci of tactile stimulation is impaired in subjects with Parkinson's disease. Clin Anat. 2003; 16:241–247. [PubMed: 12673819]

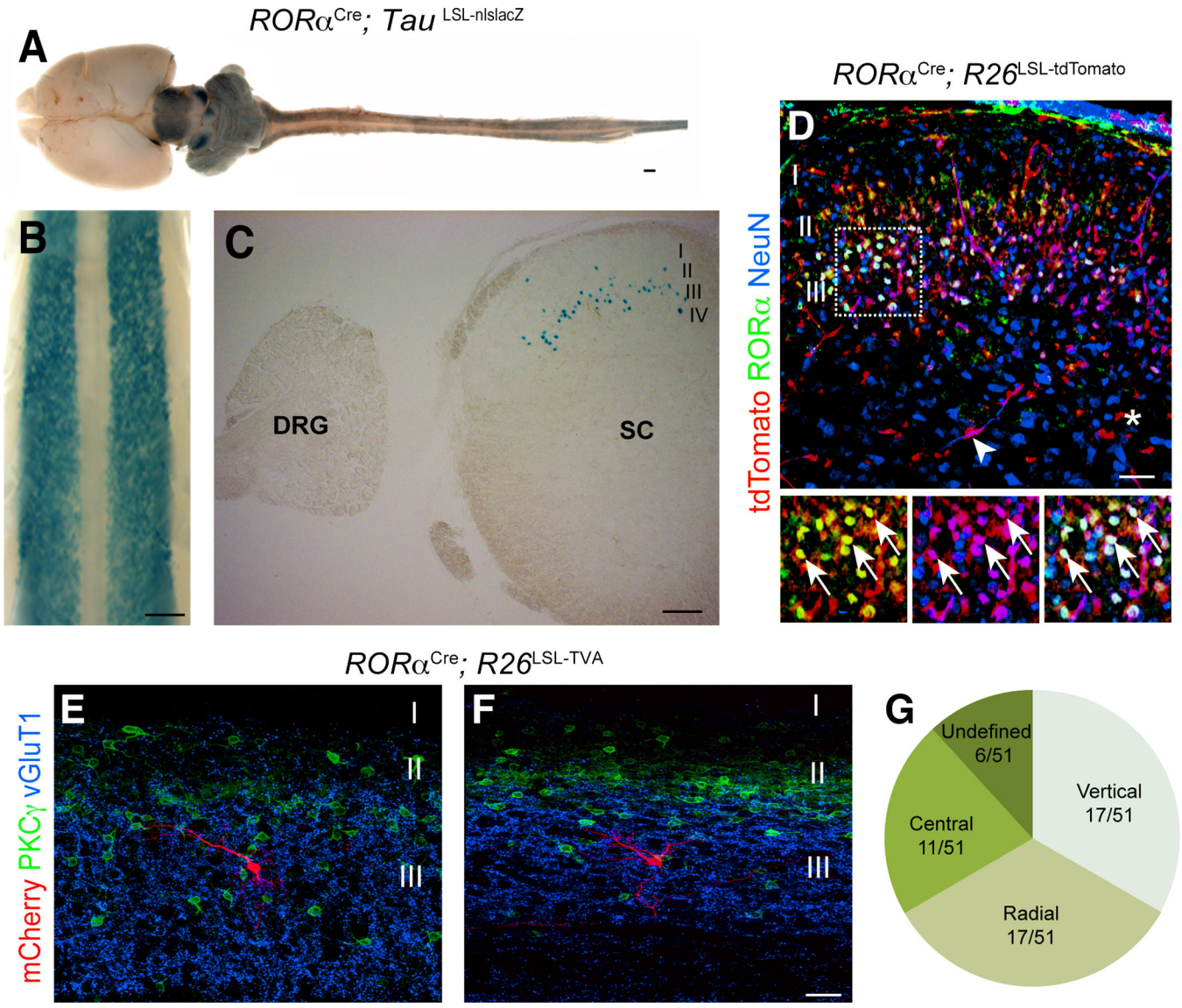

Figure 1. Characterization of *RORα*^{Cre}-derived INs in the spinal cord

(**A–C**) Images from P10 *RORα*^{Cre}; *Tau*$^{LSL\text{-}nlslacZ}$ mice showing β-galactosidase expression in the central nervous system (A) and spinal cord (B and C). C shows transverse section through the spinal cord. (**D**) Section through P10 *RORα*^{Cre}; *R26*$^{LSL\text{-}tdTomato}$ lumbar spinal cord stained with antibodies to RORα (green) and NeuN (blue). tdTomato^{+} fluorescence (red) was visualized without staining. Merged image shows tdTomato is largely restricted to RORα^{+}/NeuN^{+} neurons in lamina IIi/III. The tdTomato^{+} cells located outside of lamina II/III do not express NeuN. Arrows indicate double-labeled neurons. Arrowhead in D indicates a tdTomato^{+} blood vessel. Asterisk marks a tdTomato^{+} glial cell. (**E–F**) mCherry-labeled neurons (red) in the lumbar cord of P21 *RORα*^{Cre}; *R26*$^{LSL\text{-}TVA}$ mice. Their location in relation to excitatory PKCγ^{+} neurons (green) and vGluT1 sensory afferents (blue) is shown. (**G**) Summary of the morphological profile of 51 RORα INs. Scale bars: 1000 μm (A), 500 μm (B), 200 μm (C), 100 μm (D), 25 μm (E and F). See also Figure S1.

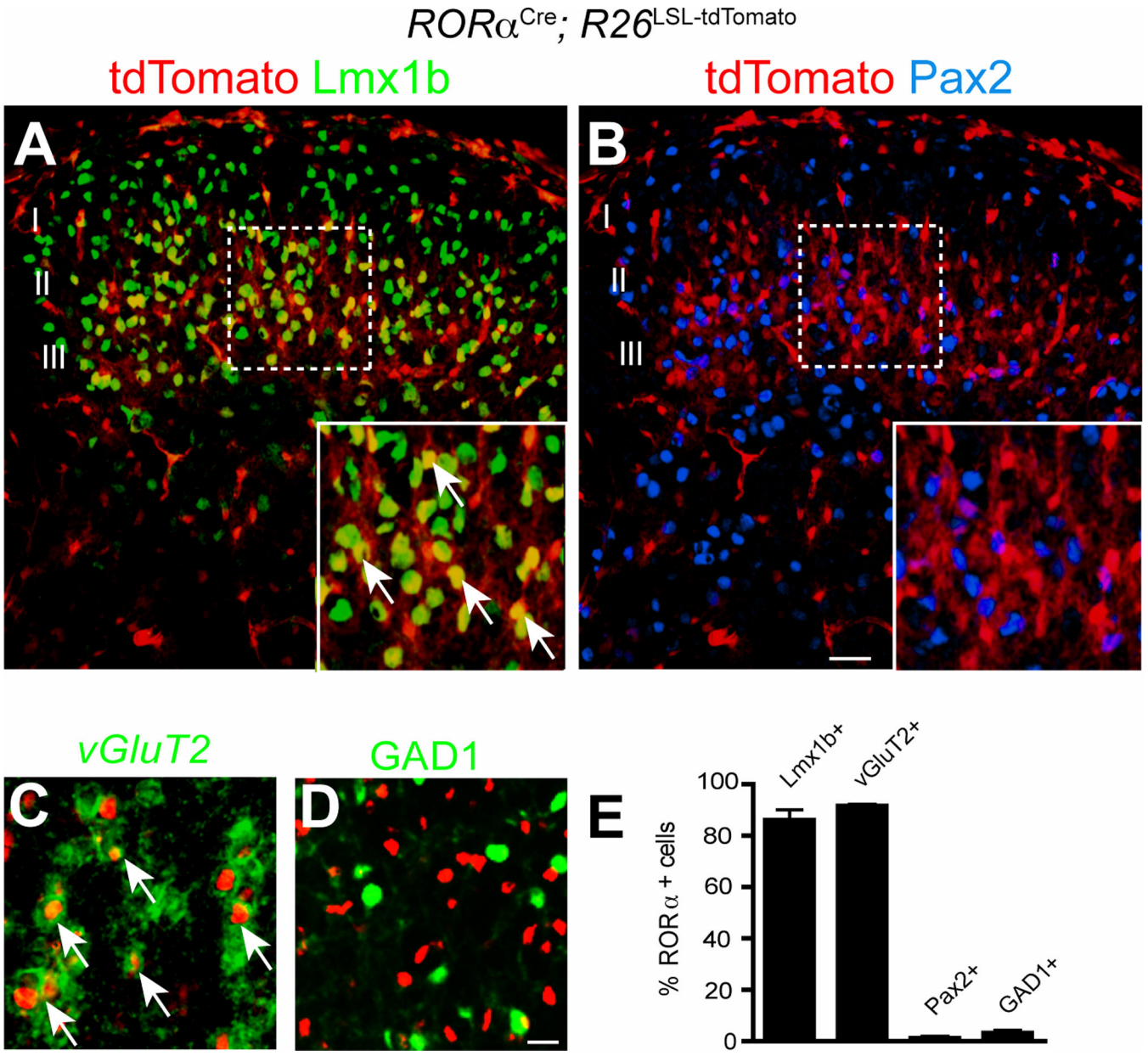

Figure 2. RORα identifies a population of excitatory interneurons in the dorsal horn of the spinal cord

(**A–B**) Transverse sections through P10 *RORα*^{Cre}; *R26*$^{LSL\text{-}tdTomato}$ lumbar dorsal spinal cord showingRORα os coexpressed with Lmx1b, but not with Pax2. (**C–D**) Sections from P10 *RORα*^{Cre}; *R26*$^{LSL\text{-}tdTomato}$; *GAD1-GFP* spinal cord showing tdTomato is coexpressed with *vGluT2* mRNA (C, green), but not GFP (D, green). (**E**) Quantification of dorsal spinal cord marker expression in RORα INs. Cell counts obtained from 3 spinal cords were pooled and expressed as mean ± SEM. Cell counts for RORα INs expressing Lmx1b (940/1093), vGluT2 (904/987), Pax2 (15/1197) and GAD1 (22/845). Scale bars: 100 μm (A–B), 10 μm (C–D). See also Figure S2

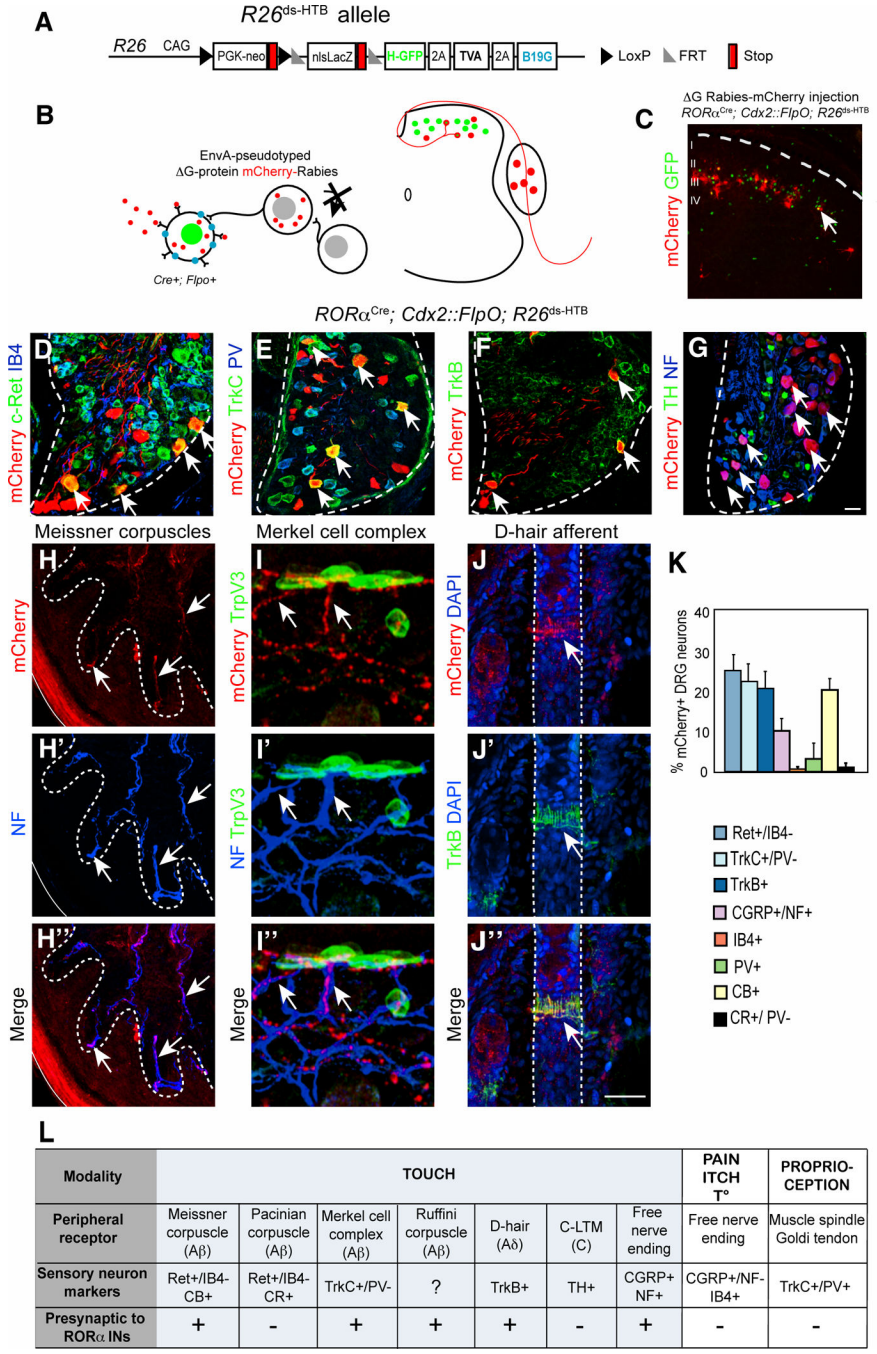

L

Modality	TOUCH							PAIN ITCH T°	PROPRIO-CEPTION
Peripheral receptor	Meissner corpuscle (Aβ)	Pacinian corpuscle (Aβ)	Merkel cell complex (Aβ)	Ruffini corpuscle (Aβ)	D-hair (Aδ)	C-LTM (C)	Free nerve ending	Free nerve ending	Muscle spindle Goldi tendon
Sensory neuron markers	Ret+/IB4-CB+	Ret+/IB4-CR+	TrkC+/PV-	?	TrkB+	TH+	CGRP+ NF+	CGRP+/NF-IB4+	TrkC+/PV+
Presynaptic to RORα INs	+	-	+	+	+	-	+	-	-

Figure 3. Transsynaptic rabies virus tracing of sensory inputs to RORα INs

(**A–B**) Schematic showing the *R26*$^{ds\text{-}HTB}$ allele and strategy used for tracing monosynaptic inputs to the RORα INs using an EnvA-pseudotyped ΔG-mCherry-rabies virus. (**C**) Section through P10 *RORα*^{Cre}; *Cdx2::FlpO; R26*$^{ds\text{-}HTB}$ spinal cord showing mCherry-rabies virus labbled cells and RORα INs (green). mCherry^{+}/GFP^{-} cells represent transynaptically-labeled presynaptic neurons. (**D–G**) Sections from P10 *RORα*^{Cre}; *Cdx2::FlpO; R26*$^{ds\text{-}HTB}$ lumbar DRG showing presynaptically labeled sensory neurons and sensory neuron subtype markers as indicated (**H**) Section of hindlimb footpad stained with antibodies to mCherry

(red) and NF (blue) showing Meissner corpuscles innervation. (**I**) Section of hindlimb hairy skin stained with antibodies to mCherry (red), NF (blue) and TrpV3 (green), which recognizes Merkel cells. (**J**) Section of hairy skin showing a D-hair afferent following staining with antibodies to mCherry (red), TrkB (green) and DAPI (blue) (**K**) Quantification of sensory neuronal markers in relation to total number of $mCherry^+$ neurons, n = 3 mice. (**L**) Summary of sensory afferent types that are presynaptic to the RORα INs. Abbreviations: NF, neurofilament; CB, calbindin; CR, calretinin; TH, Tyrosine Hydroxylase. Dashed lines define the boundary of the DRG (D–G) and hair follicles (J). Arrows indicate double-labeled neurons or sensory afferents. Scale bar: 50 μm (D–G), 25 μm (H–J). See also Figure S3.

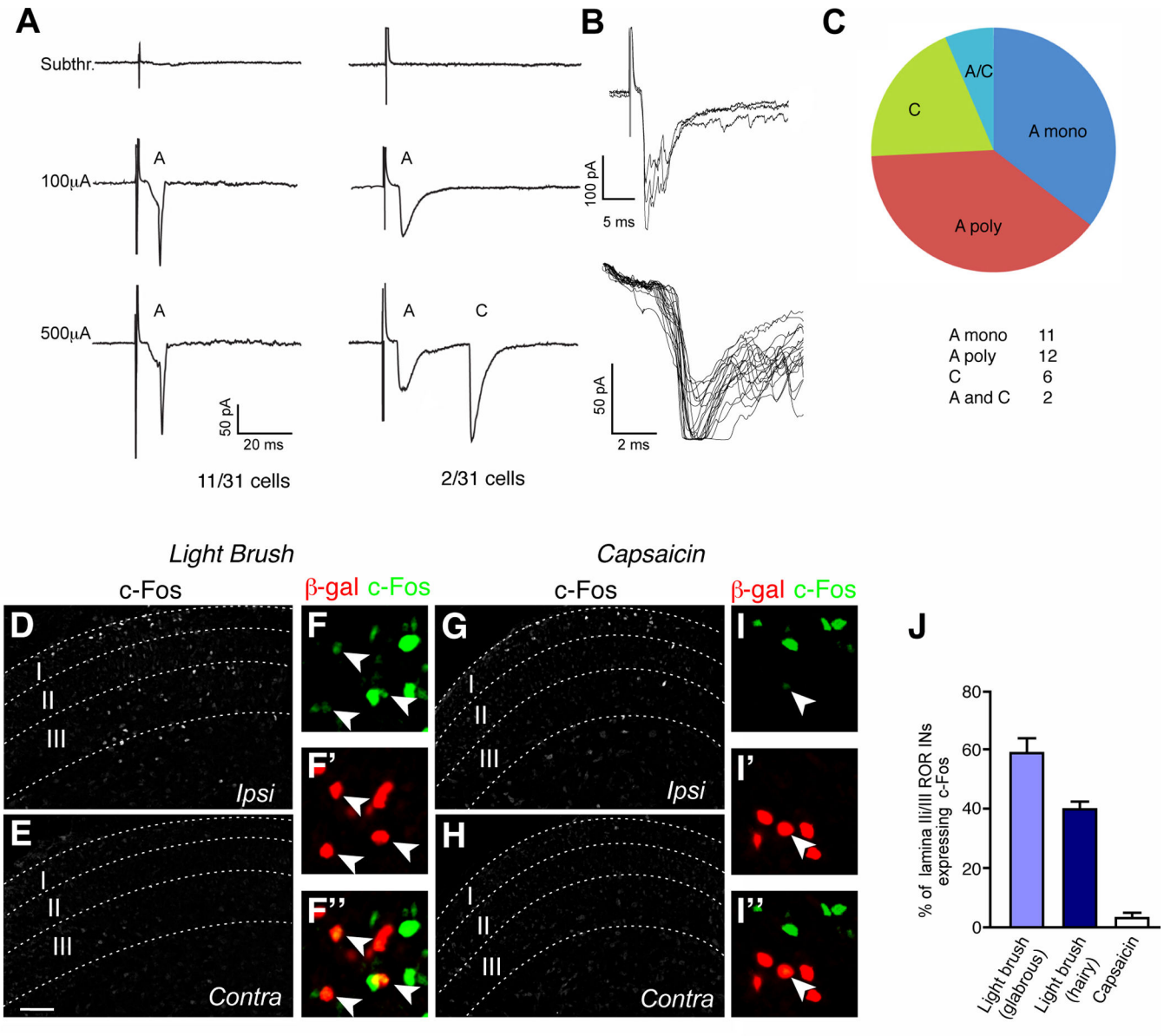

Figure 4. RORα INs are functionally innervated by low threshold mechanosensory afferents

(**A**) Example of a RORα IN in L4 displaying an A fiber monosynaptic current triggered by low intensity stimulus. Monosynaptic connectivity was confirmed by a 2Hz frequency stimulation. (**B**) Example of a RORα IN with dual A and C inputs. (**C**) Classification of potentials in RORα INs induced by dorsal root stimulation. n = 31 cells. (**D–I**) Sections through the lumbar spinal cord of P6 *RORα*^{Cre}; *R26*$^{ds\text{-}HTB}$ mice stained with antibodies to c-Fos and β-gal after light brushing (D–F) or injecting capsaicin into the footpad (G–I). Arrowheads in F and I indicate c-Fos^{+} RORα INs. Scale bars: 50 μm. Panels E and H show the contralateral side. (**J**) Fraction of RORα INs (β-gal^{+}) coexpressing c-Fos. Only lamina IIi/III cells located within the domain displaying elevated c-Fos expression were counted. Cell counts of RORα INs exhibiting c-Fos immunoreactivity: brush stimulation of glabrous skin, 1593/2830 RORα cells; brush stimulation of hairy skin, 834/2103 RORα cells;

capsaicin injection, 20/711 RORα cells. n = 4 animals for each experiment. Data: mean ± SEM. Scale bar: 100 μm (D,E,G,H).

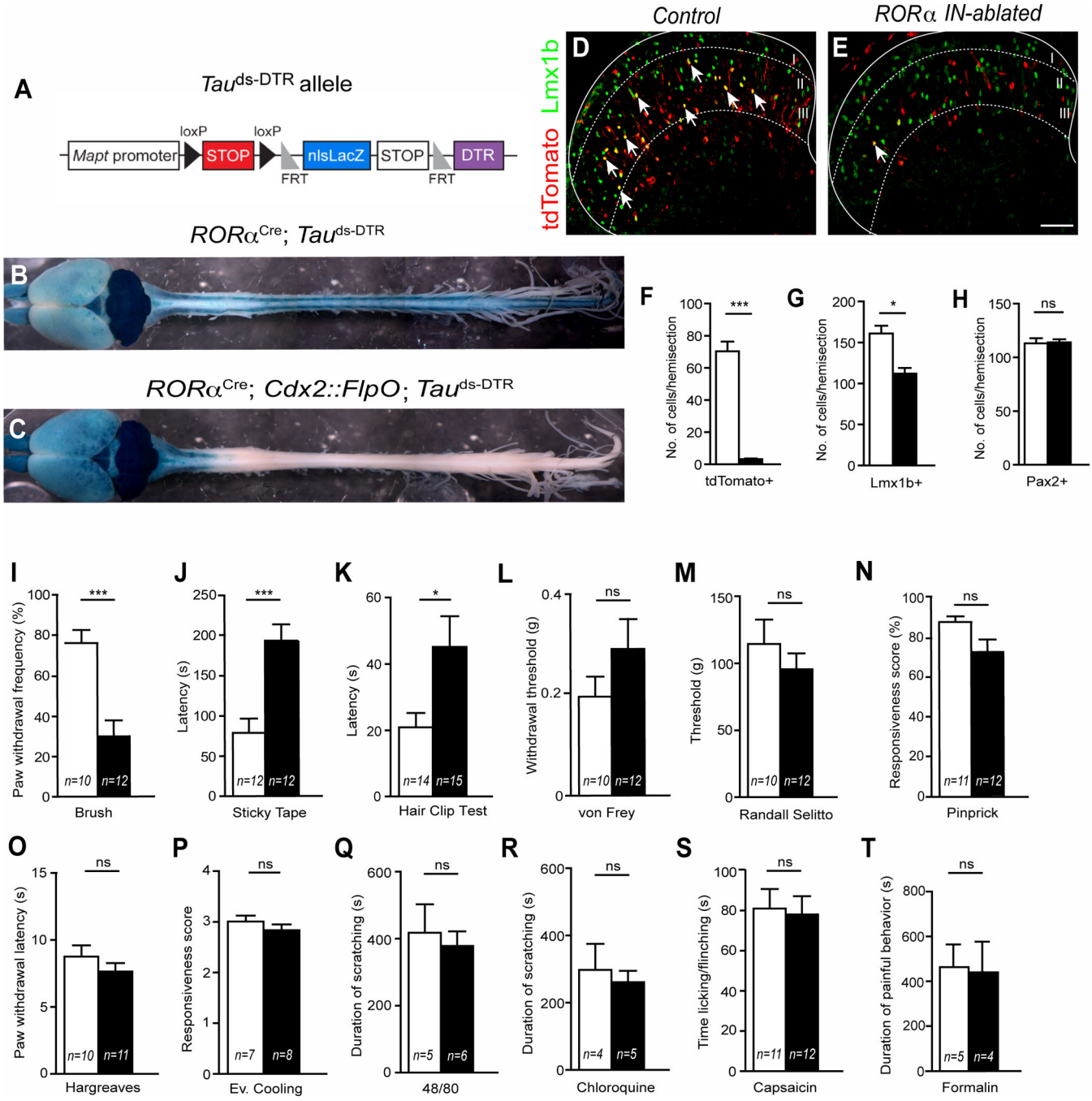

Figure 5. Spinal ablation of RORα INs impairs touch but not nociceptive behaviors

(**A**) Schematic illustrating the *Tau*$^{ds\text{-}DTR}$ allele. (**B–C**) Brain and spinal cords from P84 *RORα*^{Cre}; *Tau*$^{ds\text{-}DTR}$ (control) and *RORα*^{Cre}; *Cdx2::FlpO*; *Tau*$^{ds\text{-}DTR}$ (RORα IN-ablated) mice showing β-galactosidase reporter expression. (**D–E**) Transverse sections through the lumbar dorsal horn of adult control (D) and RORα IN-ablated (E) mice 14 days after injecting DTX showing tdTomato (red) and Lmx1b (green) expression. Arrows indicate double-labeled neurons. (**F**) RORα^{+} IN numbers are reduced by 95% following DTX-ablation (3.16±0.46 cells versus 70.30±6.01 cells), *** p<0.001. (**G**) Lmx1b-expressing

cells are reduced by 30% in RORα IN-ablated cords (112.1±6.9 cells versus 161.0±9.5 cells), * $p < 0.05$. (**H**) $Pax2^+$ cell numbers are unchanged in RORα IN-ablated cords (113.1±4.7 cells versus 113.9±2.9 cells), $p > 0.05$. (**I**) RORα IN-ablated mice show a significant decrease in paw withdrawal to dynamic light brush (30±7.9% versus 76±6.5% of trials, *** $p < 0.001$). (**J–K**) RORα IN-ablated mice show a significant increase in latency) to static light touch as measured using the sticky tape test (J, 192.9±20.4 secs versus 78.9 ± 17.7 secs, *** $p < 0.001$) and detecting a 1.5mm alligator clip on the hairy skin (K, 47.3 ± 11.5 to 20.9 ± 4.2, * $p < 0.05$). (**L–N**) Mechanical pain measured by von Frey filament, Randall Selitto and pinprick does not differ between control and RORα IN-ablated mice. (**O–R**) Sensitivity to heat (Hargreaves) and cooling (acetone) in RORα IN-ablated mice is normal, as are responses to 48/80 and chloroquine. (**S–T**) Chemical pain induced by injecting capsaicin or formalin into the footpad is also unchanged in RORα IN-ablated mice. Data: mean ± SEM. ns, p values above 0.05 are not significant. n = number of mice tested. Scale Bar: 100 μm. See also Figure S4.

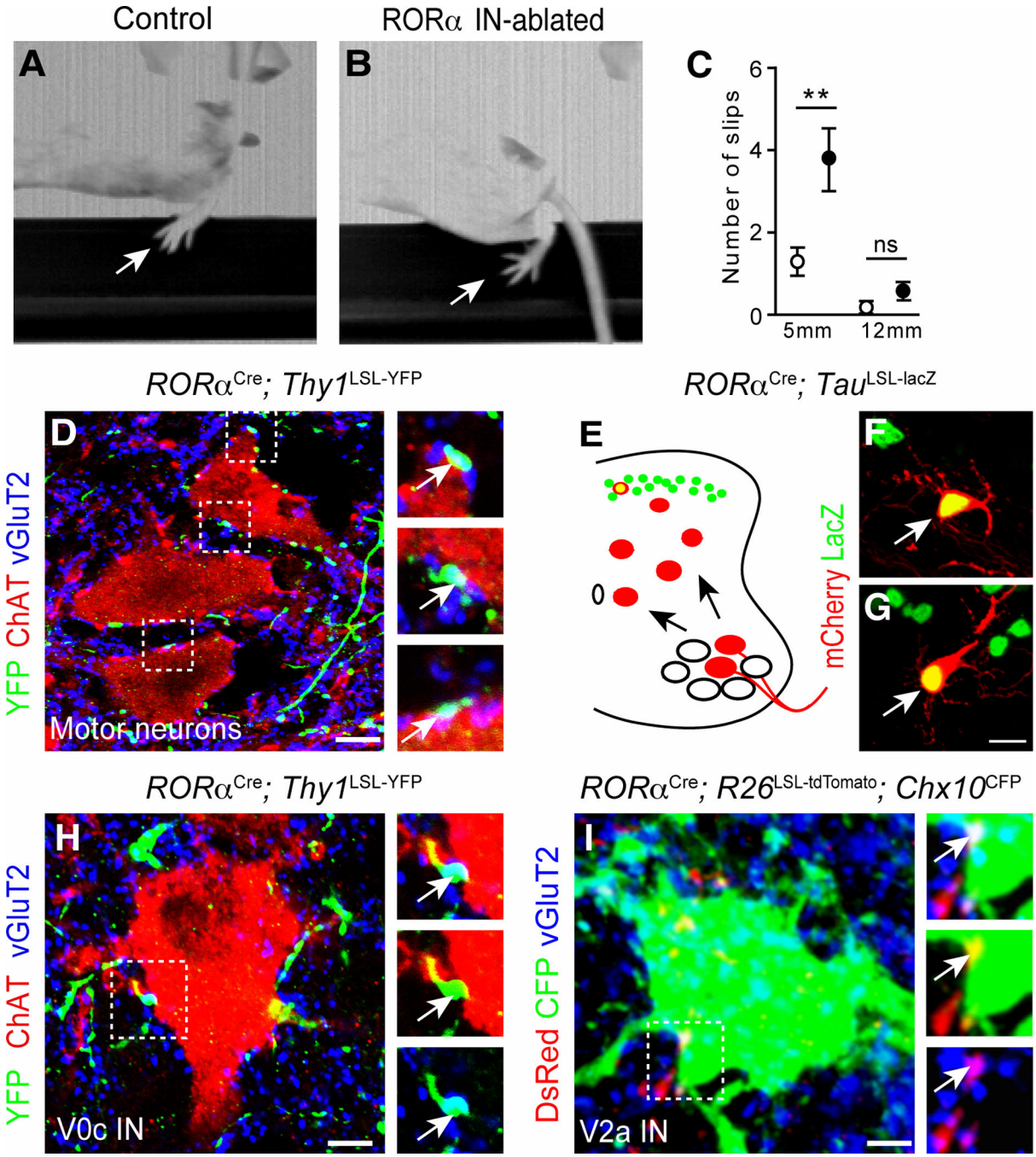

Figure 6. Corrective movements are impaired in RORα IN-ablated mice

(**A–B**) Images showing control (A) and RORα IN-ablated (B) mice crossing a 5mm wide beam. Arrow indicates position of the foot. Note the position of the foot in B showing a foot slip (**C**) Number of slips and footfalls for 5 mm and 12 mm wide beams. White circles indicate control mice (17 and 11 mice tested for 5 and 12 mm beams, respectively). Black circles indicate RORα IN-ablated mice (19 and 12 mice tested for 5 and 12 mm beams, respectively). (**D and H**) P21 *RORα*^{Cre}; *Thy1*$^{LSL\text{-}YFP}$ spinal cord sections stained with antibodies to GFP (green), vGluT2 (blue) showing synaptic boutons (arrows) on ChAT^{+}

motor neurons (D), and ChAT^{+} V0c neurons (H). (**E–G**) Retrograde monosynaptic mCherry-rabies virus labeling of RORα INs following injection into the tibialis anterior (F) and gastrocnemius muscles (G). The tracing protocol is shown in E. (**I**) P21 *RORα*^{Cre}; *R26*$^{LSL\text{-}tdTomato}$; *Chx10*^{CFP} spinal cord section stained with antibodies to DsRed (red); GFP (green) and vGluT2 (blue), showing synaptic boutons (arrows) on a Chx10^{+} V2a IN (green). Data: mean ± SEM, ** p <0.01, ns, p> 0.05 Scale bars: 5 μm (D), 10 μm (F–G), 2 μm (H,I). See also Figure S5.

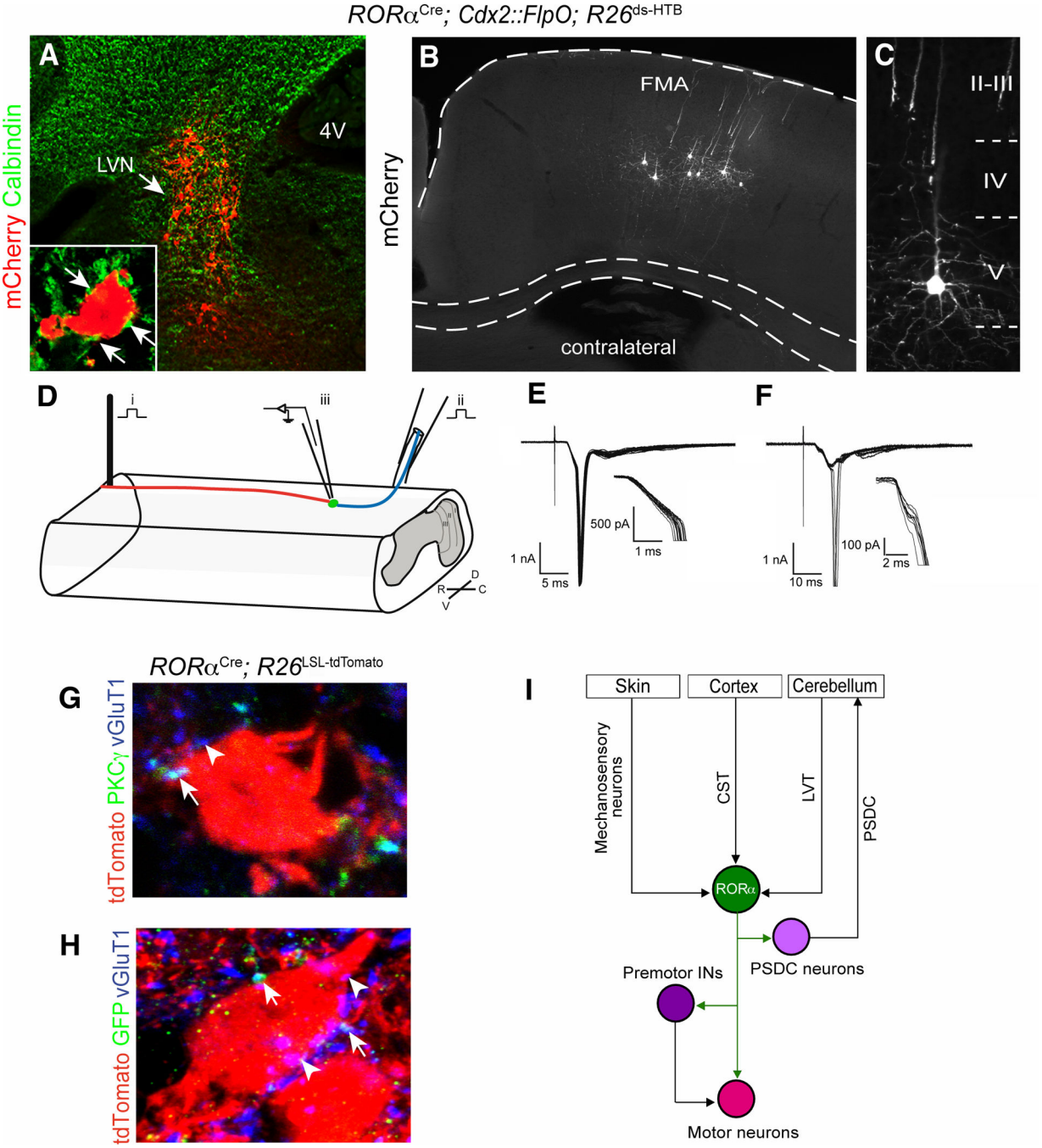

Figure 7. Convergence of sensory and descending inputs onto RORα INs

(**A–C**) Transverse sections from a P15 *RORα*^{Cre}; *Cdx2::FlpO; R26*$^{ds\text{-}HTB}$ brain 5 days after infecting RORα INs in the lumbar cord with an EnvA G-deleted rabies–mCherry virus. Transsynaptically labeled neurons (red) in the lateral vestibular nucleus (LVN) are innervated by calbindin^{+} Purkinje cells afferents (green, A). Pyramidal neurons in the frontal motor cortex area are transsynaptically labeled (B and C). (**D**) Hemicord preparation showing the stimulation-whole patch recording set-up for RORα INs. The region of the dorsal funiculus that contains corticospinal axons was stimulated with a concentric bipolar

electrode 5 segments (3–4 mm) rostral to the recorded cell (**i**). A single dorsal root (L4-L6) was stimulated with a glass suction electrode (**ii**). RORα cells (green) in L4 were patched and EPSCs were recorded (**iii**). R, rostral; C, caudal; D, dorsal; V, ventral. (**E**) Representative recording of an A fiber-type dorsal root evoked potential in a RORα IN. Magnification of onset is shown. (**F**) Putative corticospinal tract evoked EPSCs in the RORα IN that is shown in E. Latency and jitter properties are consistent with monosynaptic connectivity (see magnification of onset). (**G**) Section from a P21 *ROR*α^{Cre}; *R26*$^{LSL\text{-}tdTomato}$ spinal cord showing PKCγ^{+}/vGluT1^{+} corticospinal processes contacting a RORα IN (red). Arrow indicates a PKCγ^{+}/vGluT1^{+} corticospinal-derived synaptic bouton. Arrowhead indicates a vGluT1^{+} sensory contact. (**H**) Section from a P21 *ROR*α^{Cre}; *R26*$^{LSL\text{-}tdTomato}$; *Emx1*^{GFP} spinal cord stained with antibodies to DsRed (red), GFP (green) and vGluT1 (blue), which confirms GFP^{+}/vGluT1^{+} corticospinal contacts (arrows) onto RORα INs (red). Arrowhead indicates a vGluT1^{+} sensory contact. (**I**) Schematic showing the RORα IN connectivity and an outline of the RORα IN spinal circuit for light touch. NB. Arrows to and from the cerebellum do not indicate direct connections. Scale bar: 2 μm (G,H). See also Figure S6.